Structure and Mechanism of the Lactose Permease of *Escherichia coli*

Jeff Abramson,[1] Irina Smirnova,[3] Vladimir Kasho,[3] Gillian Verner,[3] H. Ronald Kaback,[3]* So Iwata[1,2]*

Membrane transport proteins that transduce free energy stored in electrochemical ion gradients into a concentration gradient are a major class of membrane proteins. We report the crystal structure at 3.5 angstroms of the *Escherichia coli* lactose permease, an intensively studied member of the major facilitator superfamily of transporters. The molecule is composed of N- and C-terminal domains, each with six transmembrane helices, symmetrically positioned within the permease. A large internal hydrophilic cavity open to the cytoplasmic side represents the inward-facing conformation of the transporter. The structure with a bound lactose homolog, β-D-galactopyranosyl-1-thio-β-D-galactopyranoside, reveals the sugar-binding site in the cavity, and residues that play major roles in substrate recognition and proton translocation are identified. We propose a possible mechanism for lactose/proton symport (cotransport) consistent with both the structure and a large body of experimental data.

Transport proteins, an important class of integral membrane proteins, are classified into two subsets. One subset—the major facilitator superfamily (MFS) transporters (*1*), including the lactose permease of *E. coli* (LacY) (*2*)—transduces the free energy stored in an electrochemical proton gradient into substrate concentration gradients. Another subset of transport proteins [P-type adenosine triphosphatases (ATPases) and ABC transporters] uses the energy released from ATP hydrolysis to drive solute accumulation or efflux. In contrast, channel proteins—a third important class of membrane proteins—do not transduce energy but function as selective pores that often open in response to a specific stimulus, allowing movement of solute down an electrochemical ion gradient (*3*). Like channels, membrane transport proteins are highly relevant to human physiology and disease (e.g., depression, stroke, diabetes, multidrug resistance). Moreover, two of the most widely prescribed drugs in the world—fluoxetine (Prozac) and omeprazole (Prilosec)—are targeted to membrane transport proteins. Gene sequencing and hydropathy profiling indicate that members of each subset appear to have similar secondary structures (*1*), and it seems likely that their tertiary structures and mechanisms have been preserved throughout evolution.

LacY is encoded by the *lacY* gene, the second structural gene in the *lac* operon (*4*), and is solely responsible for all the translocation reactions catalyzed by the galactoside transport system in *E. coli* (*2*). LacY is a particularly well-studied representative of the first subset of membrane transport proteins and a member of the oligosaccharide/proton symport subfamily of the MFS transporters. Like many MFS members, LacY couples the free energy released from downhill translocation of protons in response to an electrochemical proton gradient to drive the energetically uphill stoichiometric accumulation of galactosides against a concentration gradient.

The use of molecular biological approaches to engineer LacY for site-directed biochemical and biophysical studies has provided useful information about both structure and mechanism (*2, 5*). In addition to other site-directed mutants, functional LacY devoid of eight native cysteine residues (C-less LacY) has been constructed and used for cysteine-scanning mutagenesis (*5*). Analysis of the mutants yielded the following observations: (i) Only six side chains are irreplaceable with respect to active transport: Glu^{126} and Arg^{144}, which are crucial for substrate binding; Glu^{269}, which may be involved in both substrate binding and proton translocation; and Arg^{302}, His^{322}, and Glu^{325}, which play essential roles in proton translocation. (ii) Residues in addition to Glu^{126} and Arg^{144} that are important determinants for substrate binding and recognition have been identified. (iii) Substrate-induced changes in the side-chain reactivity with various chemical modification reagents, site-directed fluorescence, and spin-labeling suggest widespread conformation changes in the protein during the transport process. On the basis of these observations, a model for the transport mechanism has been postulated (*2*). Moreover, a possible three-dimensional structural model has been proposed from the results of thiol cross-linking experiments and engineered Mn(II) binding sites (*6*).

A mutant of LacY ($Cys^{154} \rightarrow Gly$, C154G) has been shown to be arrested in one conformation (*7*), and well-diffracting crystals of this mutant were successfully grown. In this report, we present the x-ray structure of the inward-facing conformation of this LacY mutant with bound substrate. The structure clearly shows the overall fold of LacY, which is composed of unusually distorted helices and a large water-filled internal cavity, as well as the details of the sugar-binding site and the possible residues involved in proton translocation. The structure is highly consistent with the proposed inward-facing conformation of LacY (*2*). The implications of these observations for the postulated mechanism of sugar/proton symport are discussed.

Overall structure. To obtain crystals of LacY, we used mutant C154G, which binds substrate with high affinity but catalyzes little or no transport, is thermostable, and exhibits little tendency to aggregate (*7*). These properties seem to be key for the successful crystallization of LacY (*8*). Statistics for data collection and structure determination are summarized in Table 1, and the experimental electron density map is shown in fig. S1. We solved structures with and without the high-affinity lactose homolog β-D-galactopyranosyl-1-thio-β-D-galactopyranoside (TDG). Unexpectedly, we found an unidentified disaccharide, likely to be of cellular origin, bound at the sugar-binding site of the structure without TDG. The two structures show little difference except for some minor alterations in the sugar-binding site. Therefore, we use the structure of LacY with TDG for the following discussion.

The overall structure of LacY is shown in Fig. 1, A and B. The asymmetric unit of the LacY crystal is composed of an artificial dimer, with two molecules oriented in opposite directions. The result indicates that the monomer is the functional unit of LacY, as reported previously (*9, 10*). The structures of the two monomers are almost identical, with

[1]Department of Biological Sciences, [2]Division of Biomedical Sciences, Imperial College London, London SW7 2AZ, UK. [3]Howard Hughes Medical Institute, Departments of Physiology and Microbiology, Immunology, and Molecular Genetics, Molecular Biology Institute, University of California, Los Angeles, CA 90095, USA.

*To whom correspondence should be addressed. E-mail: ronaldk@hhmi.ucla.edu, s.iwata@imperial.ac.uk

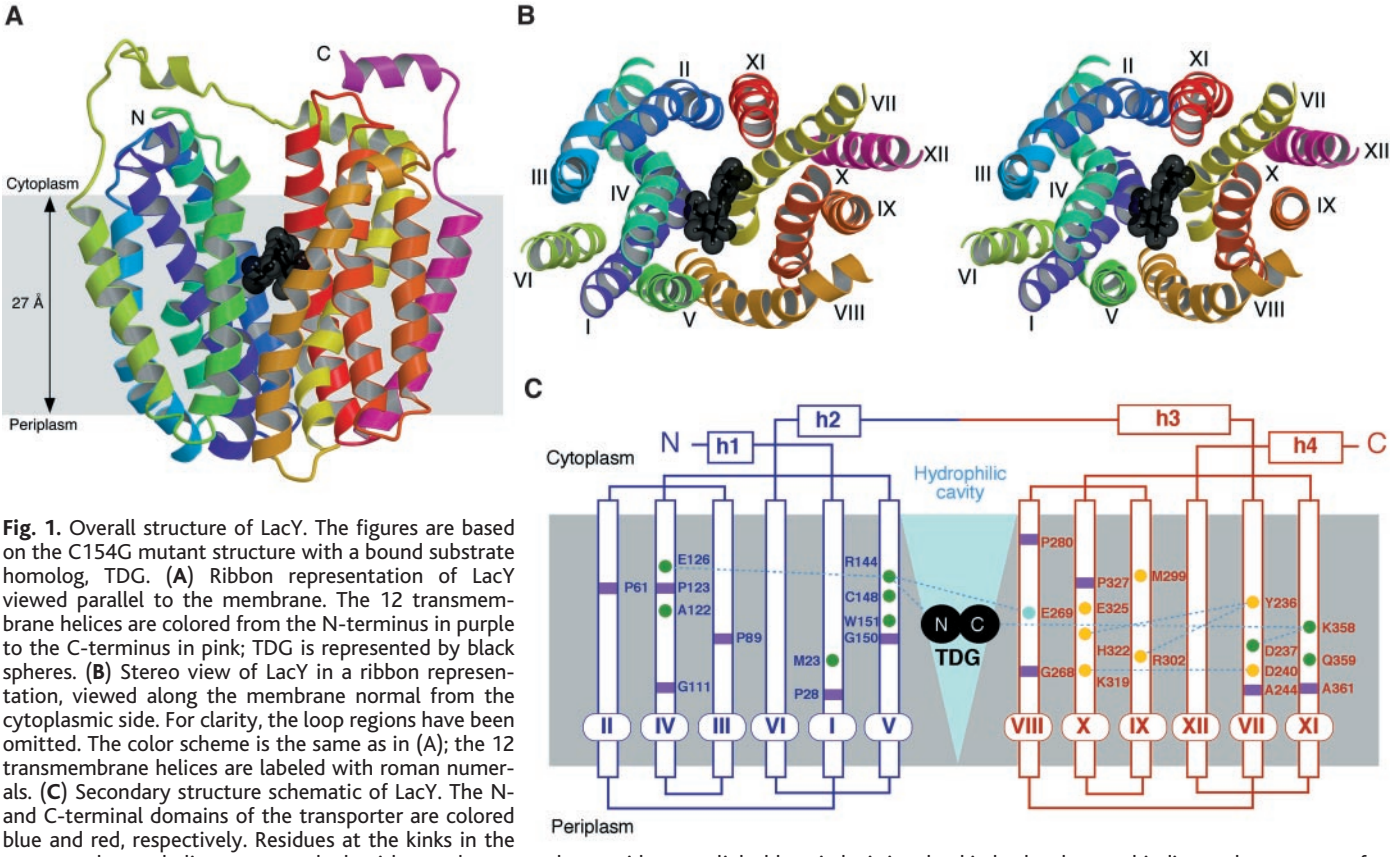

Fig. 1. Overall structure of LacY. The figures are based on the C154G mutant structure with a bound substrate homolog, TDG. (**A**) Ribbon representation of LacY viewed parallel to the membrane. The 12 transmembrane helices are colored from the N-terminus in purple to the C-terminus in pink; TDG is represented by black spheres. (**B**) Stereo view of LacY in a ribbon representation, viewed along the membrane normal from the cytoplasmic side. For clarity, the loop regions have been omitted. The color scheme is the same as in (A); the 12 transmembrane helices are labeled with roman numerals. (**C**) Secondary structure schematic of LacY. The N- and C-terminal domains of the transporter are colored blue and red, respectively. Residues at the kinks in the transmembrane helices are marked with purple rectangles; residues marked with green and yellow circles are involved in substrate binding and proton translocation, respectively; residue Glu^{269}, represented by a light blue circle, is involved in both substrate binding and proton transfer. The hydrophilic cavity is designated by a light blue triangle, and TDG is shown as two black circles; h1 to h4 denote surface helices.

a root mean square (RMS) deviation of 0.04 Å for 417 Cα atoms. Viewed parallel to the membrane, the monomer is heart-shaped with an internal cavity open on the cytoplasmic side and largest dimensions of 60 Å (along the membrane) by 60 Å (along the membrane normal). Normal to the membrane, the molecule is oval-shaped with dimensions of 30 Å by 60 Å. According to biochemical evidence (*10, 11*), the membrane is estimated to be ~27 Å (Fig. 1A). The molecule exhibits a large interior hydrophilic cavity open only at the cytoplasmic side, with dimensions of 25 Å by 15 Å, which suggests that the structure represents the inward-facing conformation (Fig. 2). Within the cavity, the TDG-binding site is found at a similar distance from both sides of the membrane, and the periplasmic side is tightly closed. This is consistent with the idea that LacY has only one binding site that is alternately accessible to each side of the membrane, as postulated 50 years ago by Widdas (*12*).

Transmembrane helix packing and domain structure. The monomer is composed of 12 transmembrane helices, as predicted (*13, 14*). The N- and C-terminal six helices form two distinct helical bundles connected by a long loop between helices VI and VII (Fig. 1C). Although loop VI/VII has two short helical segments at the N- and C-termini, it is an extended and flexible structure. The N- and C-terminal six-helix domains have the same topology and are related by an approximate two-fold symmetry, as proposed for OxlT and other MFS transporters (Fig. 1B) (*15*). A hydrophilic cavity is formed between helices I, II, IV, and V of the N-terminal domain and helices VII, VIII, X, and XI of the C-terminal domain. Helices III, VI, IX, and XII are largely embedded in the bilayer and not exposed to solvent. The two domains can be superimposed with an RMS deviation of 2.2 Å for 149 Cα atoms, indicating that the N- and C-terminal domains are likely to have the same genetic origin, although there is low sequence homology between them (*16*).

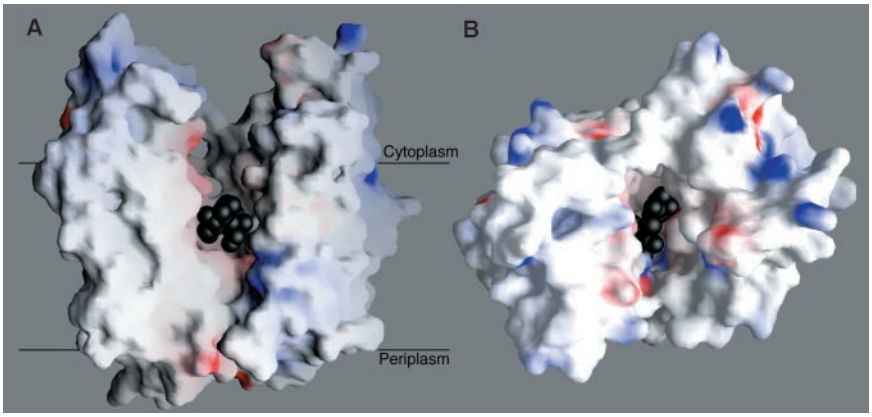

Fig. 2. The internal hydrophilic cavity of LacY. The surface model and electrostatic potential were calculated with the program GRASP (*38*). The polar surfaces are colored blue (positively charged) and red (negatively charged). The black spheres denote TDG. (**A**) View parallel to the membrane. For clarity, helices V and VIII have been removed. (**B**) View along the membrane normal from the cytoplasmic side.

Interestingly, LacY and the bacterial multidrug transporter AcrB (*17*), which is also driven by an electrochemical proton gradient, both have 12 transmembrane helices and a clear two-fold symmetry between the N- and C-terminal domains. Although the arrangement of transmembrane helices might have some similarity (except for helices I and VII), the lengths and tilt angles of the transmembrane helices in the two proteins are totally different, preventing superimposition of the structures; this indicates that they belong to different families of transporters.

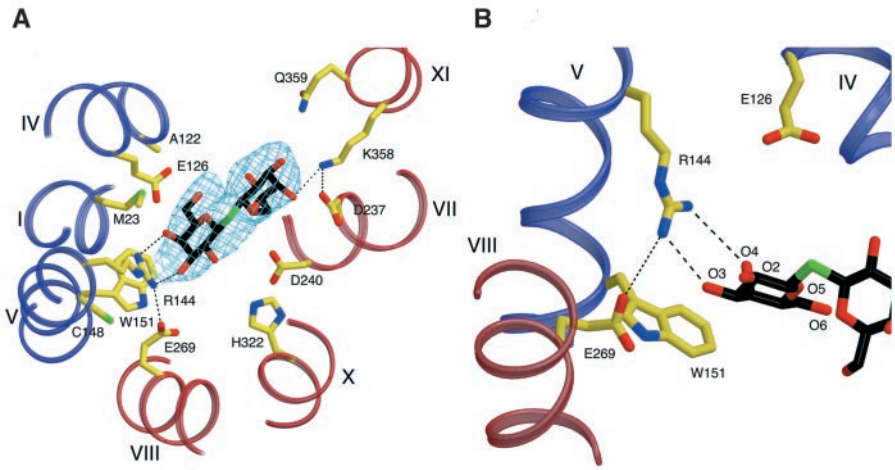

Fig. 3. Substrate-binding site of LacY. Possible hydrogen bonds and salt bridges are represented by dashed black lines. Transmembrane helices in the N- and C-terminal domains are colored blue and red, respectively. Color code for atoms: yellow, carbon in side chains; black, carbon in TDG; blue, nitrogen; red, oxygen; green, sulfur. (**A**) Residues involved in TDG binding viewed along the membrane normal from the cytoplasmic side; a $2|F_{obs}| - |F_{calc}|$ electron density map (contoured at 1.5σ) for TDG is also shown. (**B**) Closer view of the TDG-binding site in the N-terminal domain.

Table 1. Data collection, refinement, and phasing statistics for LacY structure determination. All observed reflections were used for the refinement.

Data collection and phasing

	Data set				
	Inflection	Peak	Remote	Native	TDG complex
Beamline	SLS X06SA	SLS X06SA	SLS X06SA	SLS X06SA	SLS X06SA
Wavelength (Å)	1.0088	1.0055	1.0972	1.009	0.9150
Resolution (Å)	40.0 to 3.8	40.0 to 3.8	40.0 to 4.2	40.0 to 3.5	40.0 to 3.6
Total observations	54,195	59,629	38,935	63,863	67,117
Unique reflections	22,489	22,931	16,838	25,917	26,017
Completeness (%)*	90.0 (91.2)	93.0 (93.2)	90.6 (87.2)	85.9 (71.8)	90.5 (85.6)
Redundancy	2.4	2.6	2.3	2.9	2.6
R_{sym} (%)*†	14.8 (66.9‡)	11.8 (63.0‡)	13.2 (72.7‡)	7.5 (46.1)	12.8 (44.3)
Phasing power§	1.024	1.781	—	—	—

Refinement

	Data set	
	Native	TDG complex
Resolution (Å)*	40.0 to 3.5 (3.6 to 3.5)	40.0 to 3.6 (3.7 to 3.6)
R factor (%)*‖	29.4 (35.6)	27.1 (35.3)
R_{free} (%)*¶	33.7 (37.9)	29.6 (37.3)
Average *B* values (Å^2)	51.6	49.8
RMS deviations from ideal values		
Bond length (Å)	0.012	0.013
Bond angles (°)	1.8	1.8
Dihedral angles (°)	19.6	19.6
Improper torsion angles (°)	1.0	1.1

*Values in parentheses are for the highest resolution shell. †$R_{sym} = \Sigma_h\Sigma_i|I_i(h) - \langle I(h)\rangle|/\Sigma_h\Sigma_i(h)$, where $I_i(h)$ is the *i*th measurement. ‡The last shell R_{merge} for the high-resolution set is rather high because of strong anisotropy. §Phasing power is the RMS value of F_h divided by the RMS lack-of-closure error. ‖*R* factor $= \Sigma_h||F(h)_{obs}| - |F(h)_{calc}||/\Sigma_h|F(h)|$. ¶$R_{free}$ was calculated for 5% of reflections randomly excluded from the refinement.

The substrate-binding site. The substrate-binding site is found in the hydrophilic cavity at a similar distance from either side of the membrane and in the vicinity of the approximate molecular two-fold axis of LacY (Figs. 1 and 2). The residues involved in substrate binding are shown in Fig. 3, A and B (for stereo views, see fig. S2). The two galactopyranosyl rings of TDG bind to the N- and C-terminal six-helix domains. The sugar-binding site in the N-terminal domain is composed of residues from helices I, IV, and V. In the C-terminal domain, helices VII and XI—which are symmetrically related to helices I and V, respectively—form the other half of the binding site for TDG.

The binding site in the N-terminal domain bears a striking similarity to the sites of many other galactoside-binding proteins (*18*). The primary hydrophobic interaction of the galactopyranosyl ring with the indole ring of Trp^{151} (helix V) is a common feature of galactoside-binding proteins. The C_6 atom of the galactopyranosyl ring also appears in a van der Waals contact with the Sδ atom of Met^{23} (helix I). A similar hydrophobic interaction between the C_6 atom of TDG and a histidine side chain is observed in the structure of an *E. coli* enterotoxin (*18*). An essential residue Arg^{144} (helix V) forms a bifurcated hydrogen bond with the O_3 and O_4 atoms of the galactopyranosyl ring. Another essential residue, Glu^{126} (helix IV), is in close proximity to Arg^{144}. The electron density map suggests that Glu^{126} may interact with the O_4, O_5, or O_6 atoms of TDG via water molecules, although we cannot model individual water molecules at this resolution. These results are consistent with findings that even the most conservative replacement for Arg^{144} (→ Lys; R144K) abolishes binding, and replacement of Glu^{126} with aspartate results in substantially reduced affinity (*2*). Although these residues do not form a salt bridge in the current structure, biochemical evidence (*19*–*21*) suggests that this could be formed in some states during turnover. Instead, in the structure, another essential residue, Glu^{269} (helix VIII), appears to form a salt bridge with Arg^{144} as well as a possible hydrogen bond with Trp^{151}. All replacements for Glu^{269}, with the sole exception of aspartic acid, are defective with respect to substrate binding and all translocation reactions (*22, 23*). Glu^{269} is in helix VIII in the C-terminal domain and seems to be key in providing the important energetic link between the N- and C-terminal helix domains (*24*), as discussed below.

It is well known that alkylation of Cys^{148} inactivates LacY by blocking binding and that Cys^{148} is protected from *N*-ethylmaleim-

ide (NEM) modification by LacY substrates (*2*). Similarly, alkylation of mutant Ala^{122} → Cys (A122C) with NEM or replacement with phenylalanine or tyrosine abolishes binding and transport of disaccharide substrates of LacY specifically, with little or no effect on galactose binding or transport (*25*). Cys^{148} and Ala^{122} are found in the vicinity of the N-terminal domain of the substrate-binding site, and the effects described are clearly explained by steric hindrance introduced by modification of the residues.

With regard to the contribution of the C-terminal domain to TDG binding, fewer interactions are observed. Only a single hydrogen bond is clearly observed between Lys^{358} (helix XI) and the O_4' atom of TDG. Asp^{237} (helix VII), which forms a hydrogen bond with Lys^{358}, is also in the vicinity of the O_4' atom of TDG; however, interaction seems to occur via a water molecule. Other polar residues including Gln^{359} (helix XI) may also be involved in binding through water molecules, as this is a common motif for sugar-binding proteins.

It is noteworthy that galactose itself is the most specific substrate for LacY but has very low affinity, which is increased markedly by various adducts at the anomeric carbon (*26*). Furthermore, although the C_2, C_3, and C_6 OH groups on the galactopyranosyl ring play roles in hydrogen bonding, the C_4 OH seems the most important determinant for specificity (*27*). The hydrophobic interaction between the galactopyranosyl ring and Trp^{151} is likely to orient the galactopyranosyl ring so that important hydrogen bonds with side chains in LacY can be formed (*28*). Therefore, the major portion of the substrate-binding site with respect to specificity is in the N-terminal domain, and the residues in the C-terminal domain that interact with the second galactopyranosyl ring in TDG increase affinity to disaccharide substrates but may have little to do with specificity.

Residues involved in proton translocation and coupling. Residues involved in proton translocation and coupling have been identified by characterizing the transport properties of mutants of the essential residues (Fig. 4) (*2*). Mutants of Arg^{302} (helix IX) and Glu^{325} (helix X) do not catalyze electrochemical proton gradient–driven active lactose transport. Neutral replacements for Glu^{325} or alanine and serine replacements for Arg^{302} are blocked specifically in all steps that involve net proton translocation, but they catalyze exchange and counterflow at least as well as wild-type LacY and bind ligand with high affinity. Mutants of His^{322} (helix X) or Glu^{269} (which forms part of the sugar-binding site) are blocked with respect to almost all translocation reactions and exhibit decreased affinity for sugar. These results and other evidence (*2*) strongly indicate that Glu^{325} and Arg^{302} are directly involved in proton translocation, whereas His^{322} and Glu^{269} couple proton translocation and substrate binding.

In this inward-facing conformation, we observe a complex salt bridge/hydrogen bond network composed of residues from helix VII (Tyr^{236} and Asp^{240}), helix X (Lys^{319}, His ^{322}, and Glu^{325}), and helix IX (Arg^{302}). The closest distance between this network and the sugar-binding site is more than 6 Å, indicating that the network does not have a direct interaction with the sugar-binding site; at least in this conformation Glu^{269} is a substrate ligand, as discussed, and is in close proximity to His^{322} (closest distance, 5.8 Å), but the two residues do not form hydrogen bonds in the current conformation. In turn, His^{322} forms a hydrogen bond to Tyr^{236}, which forms a hydrogen bond to Arg^{302}. However, with a small conformational change, the Glu^{269} side chain could form a hydrogen bond with His^{322}, as suggested by biochemical studies (*29, 30*). These findings suggest that Glu^{269} is the key residue to link the sugar-binding site in the N-terminal domain and the protonation site in the C-terminal domain (*24*).

Interestingly, Glu^{325} is in a hydrophobic environment surrounded by Met^{299} (helix IX), Ala^{295} (helix IX), Leu^{329} (helix X), and Tyr^{236} (helix VII). Because there is no hydrogen bond donor in the immediate vicinity, the carboxyl group is most likely protonated. This is consistent with the proposal (*2*) that the proton coupled with sugar translocation remains on Glu^{325} in the protonated inward-facing conformation with bound substrate. Protonated Glu^{325} could be stabilized by a hydrogen bond to the Sδ atom of Met^{299}; a similar glutamate-methionine interaction that stabilizes protonation of a glutamate residue has been reported for the D-proton pathway of bovine cytochrome c oxidase (*31*). A possible proton donor to Glu^{325} is His^{322}; although the two residues do not form hydrogen bonds in the current structure, small conformational changes of the side chains could facilitate this interaction (*29, 30*).

It has been suggested that Arg^{302} could interact with Glu^{325} to drive proton release from Glu^{325} because mutants of either residue exhibit the same specific defect in proton-coupled lactose translocation reactions, with no effect on sugar exchange or counterflow (*32*). In the current structure, the side chain of Arg^{302} is ~7 Å away from Glu^{325}, which would require a large side-chain rearrangement of Arg^{302} to form a salt bridge.

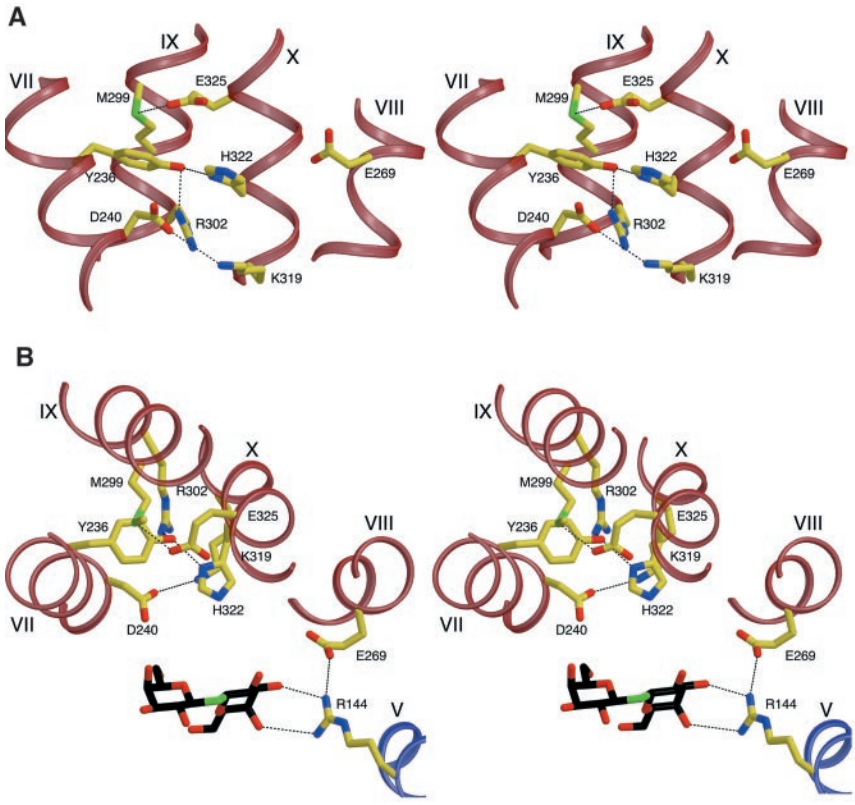

Fig. 4. Residues involved in proton translocation and coupling. Hydrogen bonds are represented by dashed black lines. Transmembrane helices in the N- and C-terminal domains are colored blue and red, respectively. Color code for atoms is as in Fig. 3. (**A**) Stereo view parallel to the membrane. (**B**) Stereo view along the membrane normal from the cytoplasmic side.

Alternatively, Glu^{325} and Arg^{302} could interact through hydrogen bonds via Tyr^{236}, which is located between the two residues.

As predicted (*5*), a salt bridge is observed between Asp^{240} and Lys^{319}. These residues are not directly involved in proton translocation; however, they could be involved in regulation and/or stabilization of the salt bridge/hydrogen bond network of the residues discussed above. Asp^{240} is in the vicinity of Arg^{302}. Although these do not directly form hydrogen bonds, Asp^{240} may stabilize the current conformation of Arg^{302} by electrostatic interaction.

Structural changes between inward- and outward-facing conformations. The crystal structure described here represents the protonated, inward-facing conformation of LacY with bound substrate. In this structure, the central hydrophilic cavity containing the sugar-binding site is open toward the cytoplasmic side only. Clearly, an alternative, outward-facing conformation open to the periplasmic side is required for substrate transport across the membrane. Because the hydrophilic cavity exists between the N- and C-terminal domains, which are connected by a flexible loop, it is reasonable to speculate that the structural change between inward- and outward-facing conformations involves rotation between the N- and C-terminal domains around the axis parallel to the membrane.

There is experimental support for this conclusion. The NEM reactivity of mutants at the periplasmic end of LacY at the N- and C-terminal domain interface is increased in the presence of ligand, which suggests that this region of LacY undergoes conformational changes that may allow access to ligand in the outward-facing conformation (Fig. 5A). As mentioned above, the crystals structure is for the C154G mutant. Gly^{154} (helix V) is at the domain interface, and mutation from cysteine seems to allow tighter packing at the interface to stabilize the inward-facing conformation.

A clue for three-dimensional modeling of the outward-facing conformation is also derived from extensive thiol cross-linking studies in which many distances were measured between positions in the N- and C-terminal domains (*6*). Many observed distances are reasonably consistent with the x-ray structure, although there is a clear tendency for the cross-linking studies to underestimate distances because cross-linking often traps cysteines when they come closest to each other (*33*). This effect is prominent for molecules such as LacY where large conformational changes are involved during turnover. Among pairs of residues on the cytoplasmic side of LacY that exhibit cross-linking, a group is observed where the distances between residues measured by cross-linking are consistently underestimated to the extent of 10 to 15 Å relative to the crystal structure. For example, on the cytoplasmic side, the distances of residues between helix V (Phe^{140}, Gly^{141}, Ala^{143}) and helix VIII (Ile^{275}, Phe^{278}, Ala^{279}) or helix X (Cys^{333}), between helix IV (Val^{125}, Ile^{129}, Arg^{134}) and helix X (Lys^{335}, Ser^{339}), and between helix XI (Tyr^{350}, Cys^{353}, Phe^{354}) and helix II (Phe^{63}, Ser^{67}) or helix IV (Ile^{129}, Arg^{134}) are all estimated to be ~9 to 10 Å by thiol cross-linking. Because the conformation of LacY is not arrested during the cross-linking experiments, discrepancy between distances may reflect fluctuations between the inward- and outward-facing conformations of the molecule (Fig. 5). To fulfill these distances observed in the thiol cross-linking experiments, helices II-IV-XI, V-VIII-X, and IV-X must be closely packed together, which is not observed in the current inward-facing conformation.

By applying a relative rotation of ~60° between the N- and C-terminal domains, we can obtain a model for the putative outward-facing conformation that satisfies the helix packing derived from thiol cross-linking (Fig. 5B) (fig. S3). The flexible loop connecting N- and C-terminal domains is compatible with this conformational change. In the model of the outward-facing conformation, the cytoplasmic halves of helices II, IV, and V in the N-terminal domain and helices VIII, X, and XI in the C-terminal domain form an interface that closes the cytoplasmic end of the hydrophobic cavity (fig. S3). Interestingly, kinks at Pro^{123} (helix IV) and Pro^{327} (helix X), which are at the domain interface in the outward-facing conformation, are in almost equivalent positions to the kinks at Pro^{28} (helix I) and Ala^{244} (helix VII) at the domain interface in the inward-facing conformation. It is likely that these kinks allow tight closure of the hydrophilic cavity ends by conferring flexibility to these helices. Each of the eight helices that form the surface of the hydrophilic cavity is heavily distorted by kinks and bends, and each also contains many proline and glycine residues commonly found in ir-

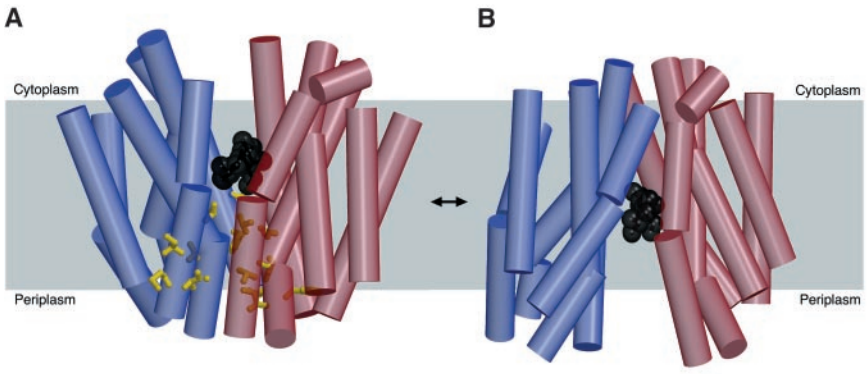

Fig. 5. Structural changes between inward- and outward-facing conformations. Transmembrane helices in the N- and C-terminal domains are shown as blue and red cylinders, respectively. (**A**) Inward-facing conformation (i.e., the crystal structure) viewed parallel to the membrane. Cysteine mutants of the residues in yellow show an increased reactivity in NEM labeling upon substrate binding. (**B**) A possible model for the outward-facing conformation, based on chemical modification and cross-linking experiments (see main text), viewed parallel to the membrane. The model was obtained by applying a relative rigid-body rotation of ~60° (around the axis passing near the TDG parallel to the membrane) to the N- and C-terminal domains.

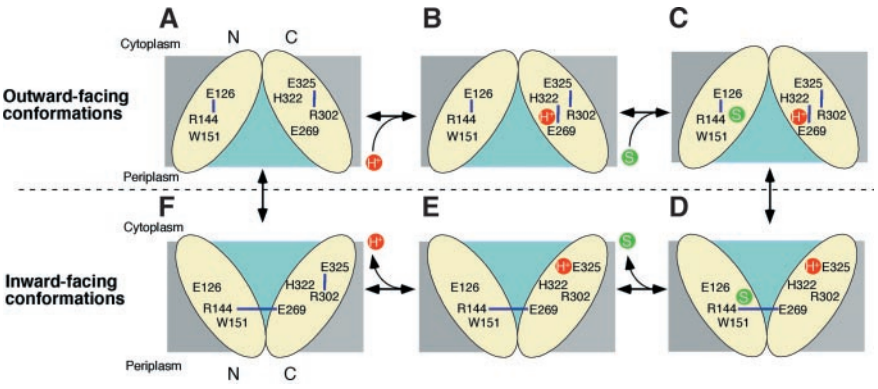

Fig. 6. A possible lactose/proton symport mechanism. N- and C-terminal domains are shown as yellow ovals. Key residues are labeled; hydrogen bonds are shown as blue lines. The proton and the substrate are shown as red and green circles, respectively; the hydrophilic cavity is represented as a light blue area.

regular helices (Fig. 1C); in contrast, helices VI, IX, and XII, which are not part of the cavity, are unperturbed. This finding implies that the irregular helices provide structural flexibility, thereby allowing the molecule to assume different conformations. The irregular shapes of many of the transmembrane helices and the dynamic conformational nature of the molecule can readily account for the very high rates and extent of H/D exchange observed with LacY (*34, 35*).

Possible mechanism of lactose/proton symport. The mechanism of lactose/proton symport is explained by a simple kinetic scheme (*2*). Influx consists of six steps starting from the outward-facing conformation, as shown in Fig. 6: (i) protonation of LacY (panels A → B); (ii) binding of lactose (B → C); (iii) a conformational change that results in the inward-facing conformation (C → D); (iv) release of substrate (D → E); (v) release of proton (E → F); and (vi) return to the outward-facing conformation (F → A). As discussed above, the structure in this paper corresponds to Fig. 6D (i.e., the protonated inward-facing conformation with bound substrate). In this structure, the relative positions of the residues are highly consistent with the proposed structure for this state, as derived from biochemical studies of various mutants (*2*). Therefore, it is likely that the proposed mechanism for lactose/proton symport based on these studies is reasonably reliable. Here, we propose a possible mechanism for lactose/proton symport that is based on biochemical studies and also fulfills the spatial requirements derived from the crystal structure (Fig. 6).

Unprotonated LacY in the outward-facing conformation (Fig. 6A) is very unstable and is protonated immediately (Fig. 6B), as postulated previously (*2*). It is suggested that in this state, the proton is on Glu^{269} or shared between Glu^{269} and His^{322}. The latter possibility is favored because Glu^{269} is totally exposed to solvent in the crystal structure. In this scenario, the conformation of His^{322} with respect to helix VIII is assumed to be different from the current x-ray structure so as to allow a hydrogen bond between His^{322} and Glu^{269} (*29, 30*). Because Arg^{144} cannot form a salt bridge with Glu^{269} in this conformation, a positive charge on Arg^{144} is likely to be stabilized by a salt bridge to Glu^{126}. Here, substrate binds to this protonated form of LacY (Fig. 6C), although it is still unclear why the substrate has a higher affinity for the protonated form. The sugar is recognized by the charge pair Arg^{144} and Glu^{126} (*19–21*), common features of sugar-binding sites.

Substrate binding induces transition to the inward-facing conformation (Fig. 6D). This is likely to be coupled with salt bridge formation between Glu^{269} and Arg^{144}, as observed in the crystal structure. The face of helix VIII with Glu^{269} has been reported to undergo a ligand-induced conformational change (*36*). A salt bridge formed between Glu^{269} from the C-terminal domain and Arg^{144} in the N-terminal substrate-binding site could induce relative rotation between N- and C-terminal domains as discussed above, resulting in the inward-facing conformation. After hydrogen bond breakage between Glu^{269} and His^{322}, the proton is transferred to Glu^{325} through the hydrogen bond to His^{322}, and the protonated Glu^{325} is stabilized in the hydrophobic environment. Substrate is then released from the inside of the membrane (Fig. 6E). This induces a conformational change in Glu^{269} within helix VIII and adjacent helices (IX, X) because the salt bridge partner Arg^{144} is released from sugar binding. At this stage, it is probable that Glu^{269} still maintains the salt bridge to Arg^{144} and the hydrogen bond with His^{322} has not yet been reformed, because the protein is still in the inward-facing conformation. This conformational change reduces the pK_a of Glu^{325} and the proton is released to the cytoplasm (Fig. 6F). Biochemical evidence strongly indicates that this deprotonation is induced by the interaction between Glu^{325} and Arg^{302} (*32*), although it is unclear from the crystal structure whether this interaction is direct or also involves Tyr^{236} (*37*). After releasing the proton, transition into the outward-facing conformation is induced (Fig. 6A). This is coupled with reformation of the hydrogen bond between Glu^{269} and His^{322}, and LacY is quickly reprotonated, resuming the ground state (Fig. 6B).

Although the proposed mechanism clearly explains how the overall conformational change of LacY could be coupled with sugar binding, many uncertainties remain with respect to the coupling of these processes and protonation/deprotonation. For example, the Arg^{302}/Glu^{325} mutants are defective in proton-coupled translocation modes in a way that is symmetrical—that is, efflux and influx (or active transport) are equally affected. This suggests that influx and efflux are functionally symmetric processes, a finding that is not easily explained given the asymmetric arrangement of the participating side chains and the vectoriality of proton translocation. It is always difficult to understand processes involving protons from crystal structures because protons cannot be visualized directly. Further biochemical and computational studies based on the crystal structure and structure determinations of the other states, particularly the outward-facing conformation(s), will facilitate our understanding of the mechanism of substrate/proton symport in LacY.

References and Notes

1. For a review, see M. H. Saier Jr., *Mol. Microbiol*. **35**, 699 (2000).
2. For a review, see H. R. Kaback, M. Sahin-Tóth, A. B. Weinglass, *Nature Rev. Mol. Cell Biol.* **2**, 610 (2001).
3. For a review, see C. Miller, *Curr. Opin. Chem. Biol.* **4**, 148 (2000).
4. For a review, see B. Müller-Hill, *The* lac *Operon: A Short History of a Genetic Paradigm* (de Gruyter, Berlin, 1996).
5. For a review, see S. Frillingos, M. Sahin-Tóth, J. Wu, H. R. Kaback, *FASEB J.* **12**, 1281 (1998).
6. P. L. Sorgen, Y. Hu, L. Guan, H. R. Kaback, M. E. Girvin, *Proc. Natl. Acad. Sci. U.S.A.* **99**, 14037 (2002).
7. I. N. Smirnova, H. R. Kaback, *Biochemistry* **42**, 3025 (2003).
8. See supporting data on *Science* Online.
9. M. Sahin-Tóth, R. L. Dunten, A. Gonzalez, H. R. Kaback, *Proc. Natl. Acad. Sci. U.S.A.* **89**, 10547 (1992).
10. L. Guan, F. D. Murphy, H. R. Kaback, *Proc. Natl. Acad. Sci. U.S.A.* **99**, 3475 (2002).
11. C. D. Wolin, H. R. Kaback, *Biochemistry* **40**, 1996 (2001).
12. W. F. Widdas, *J. Physiol*. **118**, 23 (1952).
13. D. L. Foster, M. Boublik, H. R. Kaback, *J. Biol. Chem.* **258**, 31 (1983).
14. J. Calamia, C. Manoil, *Proc. Natl. Acad. Sci. U.S.A.* **87**, 4937 (1990).
15. T. Hirai, J. A. Heymann, P. C. Maloney, S. Subramaniam, *J. Bacteriol*. **185**, 1712 (2003).
16. P. J. Henderson, *J. Bioenerg. Biomembr.* **22**, 525 (1990).
17. S. Murakami, R. Nakashima, E. Yamashita, A. Yamaguchi, *Nature* **419**, 587 (2002).
18. For example, see E. A. Merritt, S. Sarfaty, I. K. Feil, W. G. Hol, *Structure* **5**, 1485 (1997).
19. P. Venkatesan, H. R. Kaback, *Proc. Natl. Acad. Sci. U.S.A.* **95**, 9802 (1998).
20. C. D. Wolin, H. R. Kaback, *Biochemistry* **39**, 6130 (2000).
21. M. Zhao, K. C. Zen, W. L. Hubbell, H. R. Kaback, *Biochemistry* **38**, 7407 (1999).
22. M. L. Ujwal, M. Sahin-Tóth, B. Persson, H. R. Kaback, *Mol. Membr. Biol*. **11**, 9 (1994).
23. P. J. Franco, R. J. Brooker, *J. Biol. Chem*. **269**, 7379 (1994).
24. A. B. Weinglass, M. Sondej, H. R. Kaback, *J. Mol. Biol.* **315**, 561 (2002).
25. L. Guan, M. Sahin-Tóth, H. R. Kaback, *Proc. Natl. Acad. Sci. U.S.A.* **99**, 6613 (2002).
26. M. Sahin-Tóth, K. M. Akhoon, J. Runner, H. R. Kaback, *Biochemistry* **39**, 5097 (2000).
27. M. Sahin-Tóth, M. C. Lawrence, T. Nishio, H. R. Kaback, *Biochemistry* **43**, 13015 (2001).
28. L. Guan, Y. Hu, H. R. Kaback, *Biochemistry* **42**, 1377 (2003).
29. K. Jung, H. Jung, J. Wu, G. G. Privé, H. R. Kaback, *Biochemistry* **32**, 12273 (1993).
30. K. Jung, J. Voss, M. He, W. L. Hubbell, H. R. Kaback, *Biochemistry* **34**, 6272 (1995).
31. T. Tsukihara *et al*., *Science* **272**, 1136 (1996).
32. M. Sahin-Tóth, H. R. Kaback, *Proc. Natl. Acad. Sci. U.S.A.* **98**, 6068 (2001).
33. C. L. Careaga, J. J. Falke, *J. Mol. Biol.* **226**, 1219 (1992).
34. J. le Coutre, H. R. Kaback, C. K. Patel, L. Heginbotham, C. Miller, *Proc. Natl. Acad. Sci. U.S.A.* **95**, 6114 (1998).
35. J. S. Patzlaff, J. A. Moeller, B. A. Barry, R. J. Brooker, *Biochemistry* **37**, 15363 (1998).
36. S. Frillingos, H. R. Kaback, *Protein Sci.* **6**, 438 (1997).
37. P. D. Roepe, H. R. Kaback, *Biochemistry* **28**, 6127 (1989).
38. B. Honig, A. Nicholls, *Science* **268**, 1144 (1995).

39. Supported by the Biotechnology and Biological Sciences Research Council of the UK (S.I.) and in part by NIH grant DK51131:08 (H.R.K.). We thank T. Tomizaki and C. Schulze-Briese at the Swiss Light Source and D. Flot, B. Shepard, and S. McSweeney at the European Synchrotron Radiation Facility for technical assistance; members of the Iwata and Kaback laboratories for their support; B. Byrne for critically reading the manuscript; and M. Iwata for data collection. The coordinates for the native LacY and the TDG complex have been deposited in the Protein Data Bank (entries 1PV6 and 1PV7, respectively).

Supporting Online Material

www.sciencemag.org/cgi/content/full/301/5633/610/DC1
Materials and Methods
Figs. S1 to S3

19 June 2003; accepted 7 July 2003